

## Detection of Cracks in Heavy Weight Concrete Using Inner Electrical Resistivity Method

Mostafa Hassaan<sup>1\*</sup>, Mohamed Ihab ELMasry<sup>2</sup>, Nabil Hassan EL Ashkar<sup>3</sup>

<sup>1</sup>Research Assistant @ Ryerson University, Toronto –Ontario, Canada

<sup>2</sup>Professor of Structure Engineering @ AASTMT, Alexandria, Egypt

<sup>3</sup>Professor of Structure Engineering @ AASTMT, Alexandria, Egypt

DOI: [10.36348/sjce.2021.v05i09.004](https://doi.org/10.36348/sjce.2021.v05i09.004)

| Received: 18.08.2021 | Accepted: 01.10.2021 | Published: 06.10.2021

\*Corresponding author: Mostafa Hassaan

### Abstract

Nuclear power plants are considered as a vital structure in these days. Heavy weight concrete is used in radiation shielding for nuclear power plants which is characterized by high density of aggregate. Moreover, type of aggregate used in the concrete mix play an important role in obtaining heavy weight concrete. The coarse aggregate which is used in this research is hematite coarse aggregate. Small prisms were manufactured in the laboratory in order to measure the variation in electrical resistivity for heavy weight concrete prisms, one prism is uncracked and the other prism is manufactured with a vertical crack. The objective for this research paper is to detect the cracks using inner electrical resistivity for heavy weight concrete which contains hematite coarse aggregate. The two parameters which are used in detecting cracks are the percentage change in electrical resistivity and the second parameter is Decimal Logarithm Resistivity Anisotropy (DLRA). The inner electrical resistivity measurements were measured two concrete prisms by two methods, the first is linear inner electrical resistivity measurement (LIERM) and the other accurate one is the square inner electrical resistivity measurement (LIERM). This paper is concerned in detecting cracks especially the inner cracks which can't be observed by naked eyes using non-destructive testing method such as inner electrical resistivity method. It was concluded that the inner electrical resistivity can be used efficiently for detecting inner cracks using the percentage change in electrical resistivity and DLRA which detect the presence of crack inside the small laboratory prisms efficiently.

**Keywords:** Hematite Coarse Aggregate; Inner Electrical Resistivity Methods; Percentage Change in Electrical Resistivity; Decimal Logarithm Resistivity Anisotropy.

Copyright © 2020 The Author(s): This is an open-access article distributed under the terms of the Creative Commons Attribution 4.0 International License (CC BY-NC 4.0) which permits unrestricted use, distribution, and reproduction in any medium for non-commercial use provided the original author and source are credited.

### 1. INTRODUCTION

Concrete is the most widely used material for reactor shielding due to its cheapness and satisfactory mechanical properties. The aggregate components for concrete that contains a mixture of many heavy elements play an important role in improving concrete shielding properties (Mehta and Monteiro, 2006). Heavyweight and high strength concrete can be used for shielding purposes (Mehta and Monteiro, 2006). Heavyweight concrete mixes can be proportioned using the American Concrete Institute method (ACI) of absolute volumes developed for normal concrete. The absolute volume method is generally accepted and is considered to be more convenient for heavyweight concrete according to Ouda, (2014). The absolute volume method obtains denser concrete which was used in the calculation of the concrete mixtures. Concrete mixes with compressive strength more than 60 MPa

were prepared using 10% silica fume as a partial addition to OPC according to Ouda, (2014).

Electrical resistivity is considered as a non-destructive testing method for the RC elements in detecting cracks and its propagation inside the RC element (Elmasry *et al.*,2012), (Elashkar *et al.*,2012). This technique is low in cost, simple method and efficient. The electrical resistivity of concrete is related to the microstructure of the cement matrix, its pore structure, porosity, and pore size distribution. In concrete, the current flows through the pore liquid in the cement paste (Madhavi and Annamalai, 2016). Aggregate can be considered essentially inert. Conduction of electricity through concrete may take place in two ways that are electronic and electrolytic. Electrolytic occurred by motion of ions in concrete inside the pore solution, the electronic conduction

occurs through the motion of free electrons in the conductive media.

Concrete electrical resistivity is a geometry independent material property that describes the electrical resistance, the ratio between the applied voltage and the resulting current in unit cell geometry (Madhavi and Annamalai, 2016). These characteristics are controlled by the degree of hydration of the cement paste in concrete. Electrical resistivity is the inverse of electrical conductivity (Madhavi and Annamalai, 2016). One of the factors that control the electrical resistivity is the degree of hydration for the cement paste of concrete, thus resulting in an increase of electrical resistivity with respect to time. Others influential factors affecting the electrical resistivity are the relative humidity, the concrete temperature, and the ions concentration and their mobility in the pore solution (shahroodi, 2010). Presences of cracks in concrete act as a wall between the movements of these ions (Madhavi and Annamalai, 2016). Electrical conductivity can be used to detect and monitor crack initiation and propagation of cracks in concrete. The electrical resistivity of concrete can be measured by several means (Polder, 2000). Typically, electrodes are

placed on the surface and the resistance is measured. From the cell geometry, the resistivity can be calculated. The resistivity is often related to corrosion of steel reinforcement and durability performance of concrete (Ferreira and Jalali, 2010).

### **1.1. Methods of measuring the electrical resistivity of concrete**

There are different methods in measuring the electrical resistivity for concrete. Method of measurements can be either on the surface of concrete or embedded inside the concrete. The methods of measuring the resistivity on the surface are two plate electrode method, four-point electrode method and four probe square configuration. In addition, the methods of measuring the resistivity inside the concrete are linear inner electrical resistivity measurement and square inner electrical resistivity measurement.

### **1.1.1 Two Plate Electrode Method**

During testing, a low frequency electrical current passes between the two electrodes through the entire specimen while the voltage drop is measured as shown in Figure (1) (Morris *et al.*, 1996) and the resistivity is calculated from equation (1).

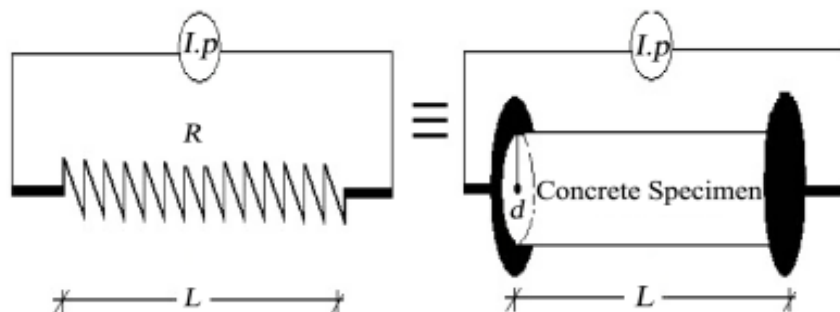


**Figure 1:** Concrete bulk electrical resistivity test with two electrodes (Morris *et al.*, 1996)

$$\rho = \frac{R A}{L} \dots \dots \dots \quad (1)$$

### 1.1.2 Four Point Electrode Method (Wenner Method)

**Method** Four-point electrode method is currently the most widely used technique for field concrete resistivity measurements. During testing, a low frequency alternating current is applied between the two outer electrodes while the voltage drop is measured in the two inner electrodes (Gowers and Millard, 1999) as shown in Figure (2) and the resistivity is calculated from equation (2). Wenner probe measurements are sensitive to the surface condition of the concrete, including the presence of moisture and voids.

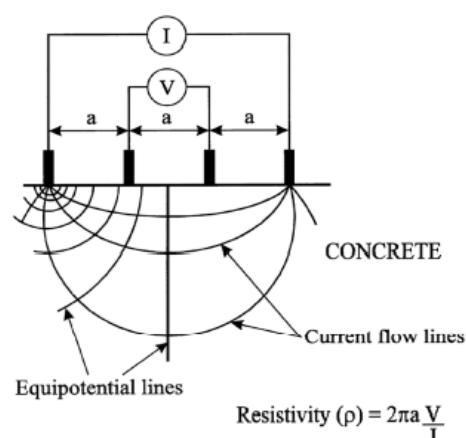


**Figure 2: Four electrode resistivity test (Gowers and Millard, 1999)**

### 1.1.3 Four probe square configuration

The four probes are arranged in a square pattern with equal spacing between electrodes as shown

in Figure (3) on the outer surface of concrete and electrical resistivity measurement can be calculated from equation (3).

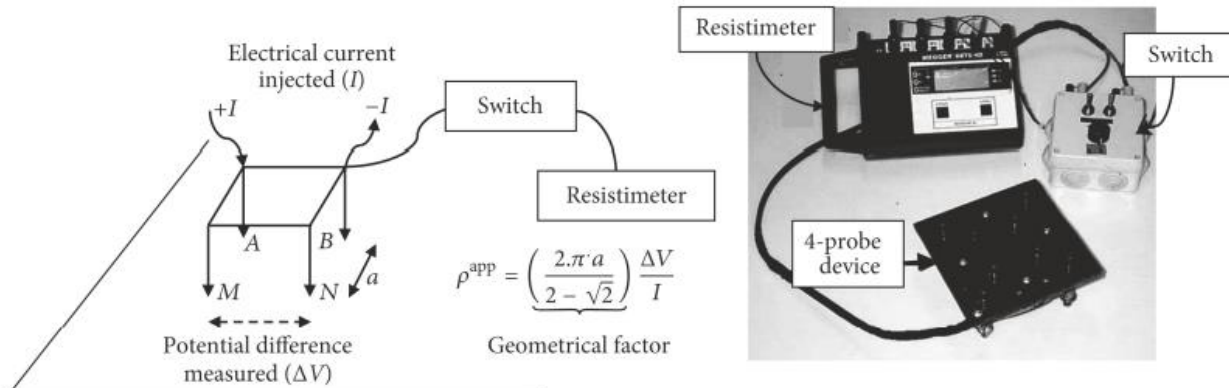


**Figure 3: Four probe square array principle (Lataste *et al.*, 2003)**

$$\rho = \frac{2 \times \pi \times a \times R}{2 - \sqrt{2}} \dots \dots \dots \quad (3)$$

#### 1.1.4 Embedded electrode configuration

#### 1.1.4.1 Linear inner electrical resistivity measurement

The four probes are arranged on the same line pattern as shown in Figure (4) inside the concrete and resistivity is calculated from equation (4) (McCarter *et al.*, 2009).



**Figure 4: Concrete cube with embedded electrodes (McCarter *et al.*, 2009)**

#### 1.1.4.2 Square inner electrical resistivity measurement

Four probes are arranged on the square pattern as shown in Figure (5) inside the concrete and resistivity is calculated from equation (5) (ElAshkar *et al.*, 2012). Four probe square measurement device has been developed by (Latoste *et al.*, 2003), for detecting cracking in reinforced concrete. This device with the square four probes can be used not only for measuring the electrical resistance with different current directions but also for measuring the material electrical anisotropy.

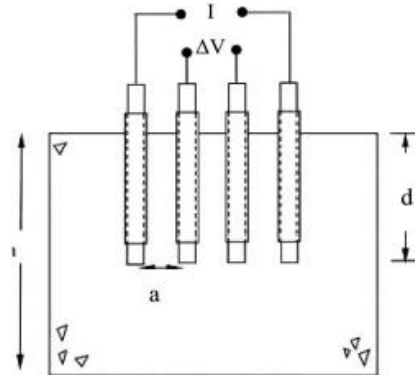


**Figure 4: Concrete cube with embedded electrodes (McCarter *et al.*, 2009)**

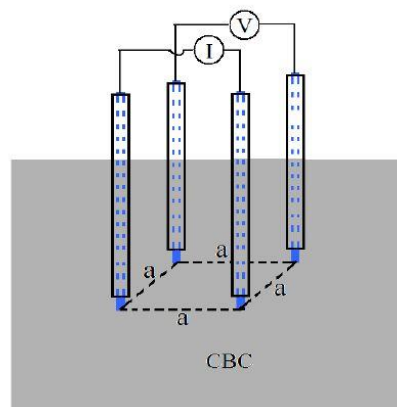


**Figure 5: SIERM Configuration (ElAshkar *et al.*, 2012)**

$$\rho = \frac{4 \times \pi \times a \times R}{2 - \sqrt{2}} \dots \dots \dots \quad (5)$$

Where:  $\rho$ : electrical resistivity (ohm.m),  $a$ : electrode spacing (m), R: resistance of electrical current (ohm), A: cross section area of specimen; and L: length of the specimen

There are two parameters for detecting damage especially the cracks inside the concrete. The parameters are percentage change in electrical resistivity and Decimal Logarithm Resistivity Anisotropy (DLRA).

- Percentage change in electrical resistivity can be calculated from equation (6) (Elmasry *et al.*, 2012), (ElAshkar *et al.*, 2012). The change in electrical resistivity would indicate a crack or may be more occurred.

$$\% \text{ Resistivity change} = \frac{R_p - R_r}{R_r} \times 100 \dots\dots\dots (6)$$

Where: Rp: resistivity at any location, Rr: reference resistivity.

- Decimal Logarithm Resistivity Anisotropy (DLRA) (Elmasry *et al.*, 2012) (ElAshkar *et al.*, 2012).

DLRA is an efficient parameter for detecting cracking introduced by (Lataste *et al.*, 2003). In addition, DLRA can be calculated from equation (7).

$$DLRA = \log_{10} \frac{R_v}{R_h} \text{ or } \log_{10} \frac{R_h}{R_v} \dots\dots\dots (7)$$

Where: Rv: resistivity at vertical current Direction, Rh: resistivity at horizontal current Direction

## 2. MATERIAL USED IN CONCRETE MIX

The materials used in concrete mix design for concrete of compressive strength of 60 Mpa are fine aggregate from local sand, hematite coarse aggregate, Portland cement Type I, water, super plasticizer and silica fume.

### 2.1. Concrete Mix Design

Experimental results revealed that, the concrete mixes containing hematite coarse aggregate along with 10% SF reached the highest compressive strength values exceeding over 60 Mpa requirements by 14 % after 28 days of curing (Ouda, 2014). The high performance concrete achieved by concrete mix have a constant water to cement ratio of 0.35, cement content of 450 kg/m<sup>3</sup> and sand to total aggregate ratio of 40 % (Ouda, 2014) as shown in Table (1).

**Table 1: Concrete ingredients used in heavy weight concrete (Ouda, 2014)**

Mix	OPC (Kg/m <sup>3</sup> )	Fine Aggregate (Kg/m <sup>3</sup> )	Hematite Coarse Aggregate (Kg/m <sup>3</sup> )	Pozzolanic Material Silica Fume (Kg/m <sup>3</sup> )	Super Plasticizer (Kg/m <sup>3</sup> )	Water (Kg/m <sup>3</sup> )
Quantity	450	909	1126	45	9.7	157.5

### 2.2 Physical Properties of Hematite Coarse Aggregate

The physical property of hematite coarse aggregate includes its unit weight, specific gravity, colour and its crushing value as shown in Table (2).

**Table 2: Physical properties of hematite coarse aggregate and the shape of hematite coarse aggregate**

Properties	Results
Specific gravity	4.17
Bulk density (Kg/m <sup>3</sup> )	2600
Particle shape	Angular
Nominal maximum aggregate size	38 mm
Colour	Black rock
% Crushing Value	19.07066
Shape of Hematite Coarse Aggregate	

### 2.2.1 Sieve analysis for hematite coarse aggregate

Sieve analysis for hematite coarse aggregate is shown in Figure (6). The specification of coarse aggregate limit is according to ESS 1109-1971 (ESS, 2002).

The grading curve for coarse aggregate is satisfied the Egyptian standard specification limit and the curve is located between upper and lower limit of specification.

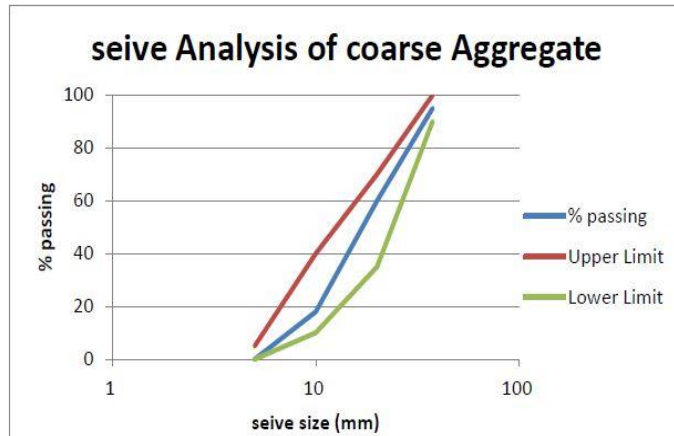


Figure 6: Sieve analysis for hematite coarse aggregate

### 2.2.2 Chemical composition for hematite coarse aggregate

The chemical composition for the hematite coarse aggregate material was conducted by using XRF spectrometer as shown in Table (3).

Table 3: Chemical composition of hematite coarse aggregate

Compound	Percentage %
Fe <sub>2</sub> O <sub>3</sub>	73.6
SiO <sub>2</sub>	10.1
MnO	0.359
CaO	6.17
MgO	9.75
Al <sub>2</sub> O <sub>3</sub>	0.021

### 2.3 Physical properties of fine aggregate

#### 2.3.1 Sieve analysis for fine aggregate

The natural sand is used as fine aggregate which has a specific gravity of 2.68. Sieve analysis of the fine aggregate is conducted as shown in Figure (7). The unit weight of the fine Aggregate is 1850 kg/m<sup>3</sup>

and the fineness modulus is 2.8. The specification of fine aggregate limit follows the ESS 1109-1971(ESS, 2002). The grading curve for fine aggregate is satisfied the Egyptian standard specification limit and the curve located between upper and lower limit.

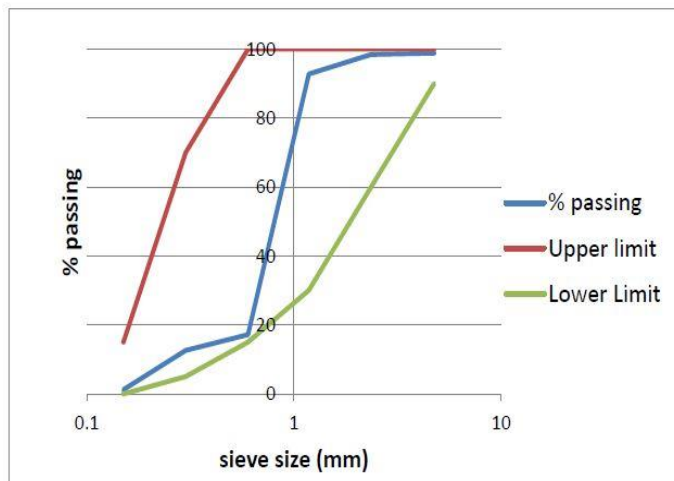
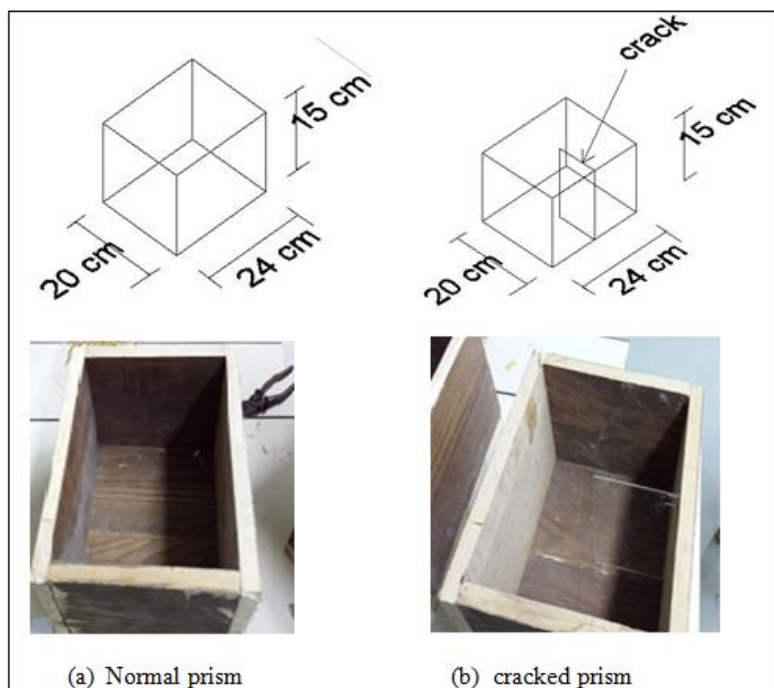


Figure 7: Sieve analysis for fine aggregate

## **2.4 Dimensions of laboratory concrete prisms**

The geometric dimension of the two prisms are ( $240 \times 200 \times 150$  mm), one of prism is uncracked and the other prism has an embedded manufactured crack as shown in Figure (8). The crack can be resembled by using plastic sheet of dimension ( $100 \times 150$  mm) of thickness 1.5mm. The electrode measures the resistance of current and the spacing between each electrode is 25 mm. The electrodes are away from the end of form

work of the prism by 30mm. The form work is manufactured from plywood which doesn't absorb the water of concrete mix. The electrodes were made of circular copper wire of diameter 1.5 mm and its length is 100mm at each end of copper wires 10mm of plastic were removed. In addition, the wire is embedded inside the concrete prism by a 50mm vertical distance as shown in Figure (9).



**Figure 8: Concrete prisms dimension**

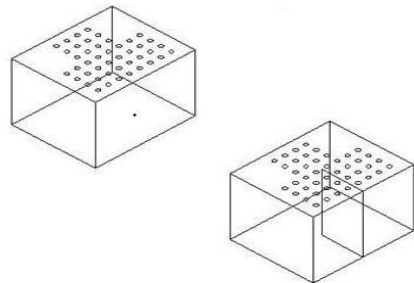


**Figure 9: Electrode spacing inside concrete prisms**

### **3. ANALYSIS OF RESULT**

The two prisms in this research were used in order to detect the variation in electrical resistivity between cracked and uncracked prisms. Moreover, there are two methods for measuring inner electrical resistivity in this research. The first method for measurement is linear inner electrical resistivity measurement, while the second one is square inner electrical resistivity measurement.

Linear inner electrical resistivity measurement was taken on several lines of two prisms with a distance of 25 mm between electrodes as shown in Figure (10). LIERM can be calculated using equation (8).

where:  $\rho$  = Electrical resistivity (ohm.m),  $a$  = electrode spacing (m),  $R$  = resistance of electrical current to pass in pore solution (ohm).

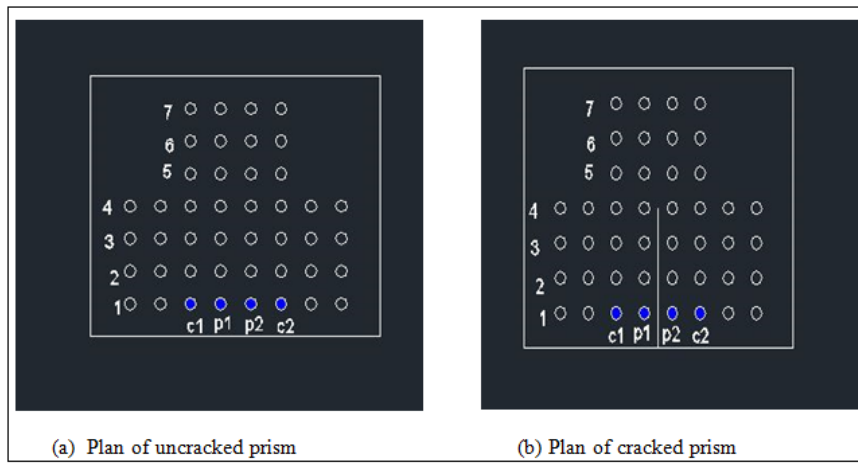


**Figure 10: LIERM configurations for different prisms with a distance between electrodes of 25mm**

Resistivity for uncracked prism in linear inner electrical resistivity measurement reached a constant

value of 192 ohm.m after 21 days as shown in Figure (11).

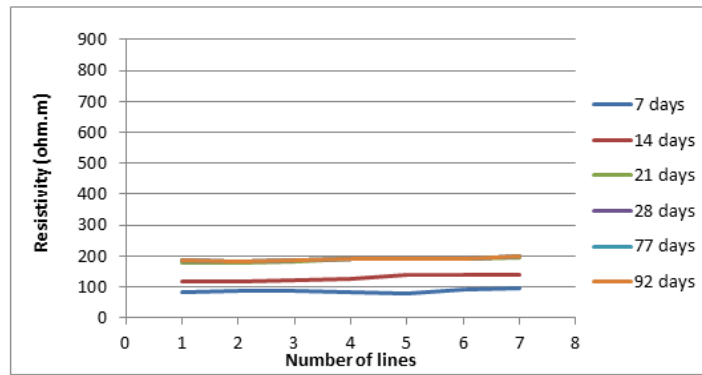


**Figure 11: Linear inner electrical resistivity measurements for uncracked prism at different ages at 25 mm electrode spacing**

Resistivity for cracked prism in linear inner electrical resistivity measurement reached a maximum value of 900 ohm.m after 21 days at the third line as shown in Figure (12) at which the crack is perpendicular to the direction of current. Moreover, the resistivity for cracked prism reached a value of 500 and 660 ohm.m at the third line of measurement at ages of 7

and 14 days respectively. After the fourth line the resistivity decreased and reached a value of 190 ohm.m after 21 days at which the current is away from the crack plane. It was observed that linear inner electrical resistivity measurement can detect and locate the presence of crack.

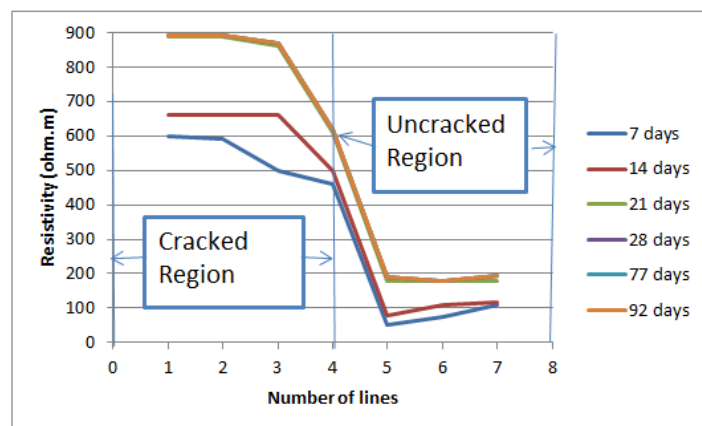


**Figure 12: Linear inner electrical resistivity for cracked prism at different ages @ 25 mm electrode spacing**

It was observed that percentage change in linear inner electrical resistivity between cracked and uncracked prism reached a value of 464%, 450% and 372% at the third line of measurement at ages of 7, 14

and 21 days respectively as shown in Figure (13). The resistivity reached a minimum value at the fifth line at which the crack is away from the current direction.

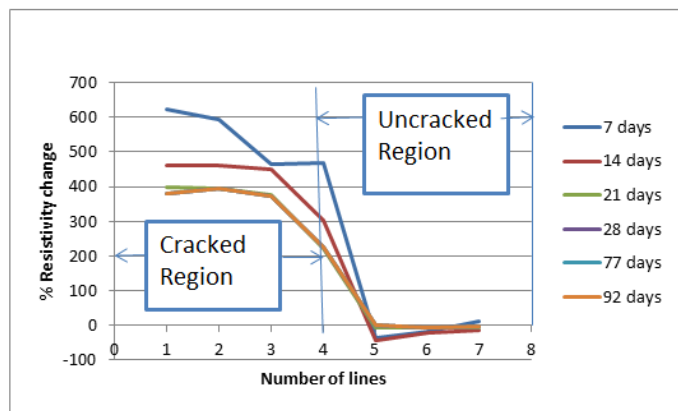


**Figure 13: Percentage change in LIERM between cracked and uncracked prisms at different ages @ 25 mm electrode spacing**

Square inner electrical resistivity measurements (SIERM) measure the inner electrical resistivity for uncracked and cracked concrete prism inside the concrete as shown in Figure (14). SIERM can be calculated from equation (9).

$$\rho = \frac{4\pi a R}{2-\sqrt{2}} \dots \dots \dots \quad (9)$$

Where:  $\rho$  : is the electrical resistivity (ohm.m), a: is the electrode spacing (m), R: resistance of current passes in concrete pore solution (ohm).

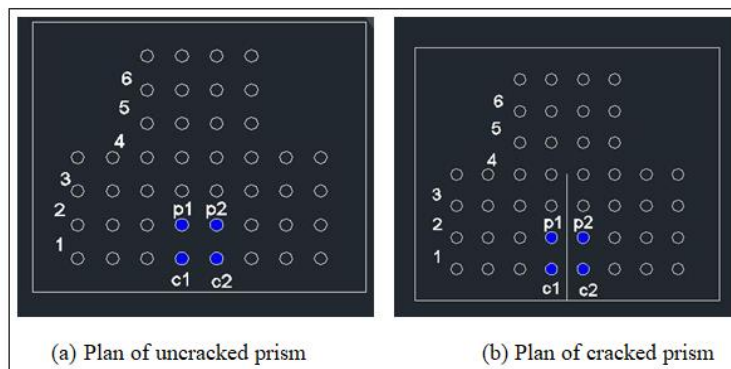


**Figure 14:** SIREM configuration for different prisms

Resistivity for uncracked prism in square inner electrical resistivity measurement reached a constant

value of 190 ohm.m after 21 days as shown in Figure (15).

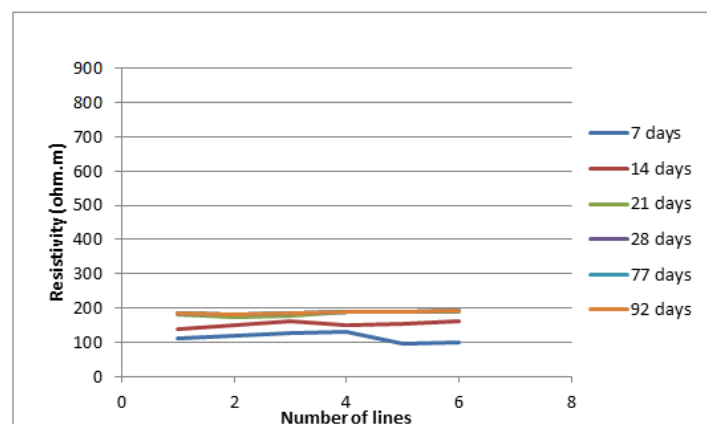


**Figure 15:** Square inner electrical resistivity measurements for uncracked prism at different ages @ 25 mm electrode spacing

Resistivity of cracked prism in square inner electrical resistivity measurement reached a maximum value of 650 and 900 ohm.m at ages of 7 and 21 days respectively at the third line as shown in Figure (16) at which the crack is perpendicular to the direction of current. After the fourth line the resistivity decreased

and reached a value of 200 ohm.m after 21 days at which the current is away from the crack plane. It was observed that from the analysis that square inner electrical resistivity measurement detects and locate the presence of crack.

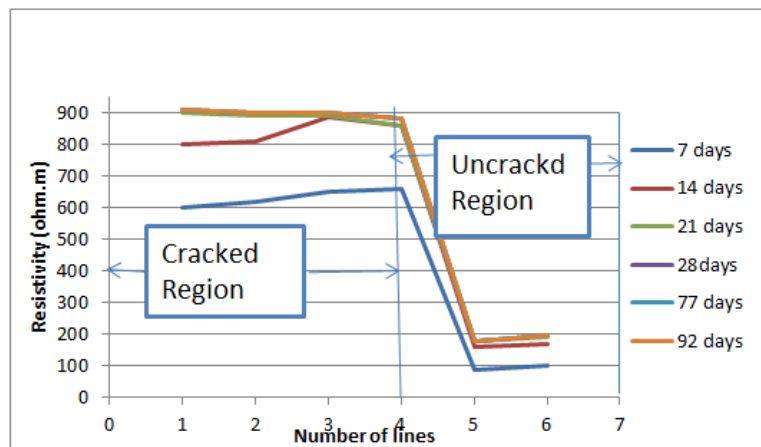


**Figure 16:** Square inner electrical resistivity measurements for cracked prism at direction perpendicular to the crack plane at different ages @ 25 mm electrode spacing

Resistivity of cracked prism in square inner electrical resistivity measurement reached a maximum value of 60 ohm.m after 21 days at the third line as shown in Figure (17) at which the crack is parallel to the direction of current. After the fourth line the resistivity increased and reached a value of 200 ohm.m after 21 days at which the current is away from the

crack plane. It was observed that from the analysis that square inner electrical resistivity measurement can detect, locate and quantify the presence of crack. The SIERM gives also the direction of the crack according to the measurement direction of square inner electrical resistivity with respect to the crack plane.

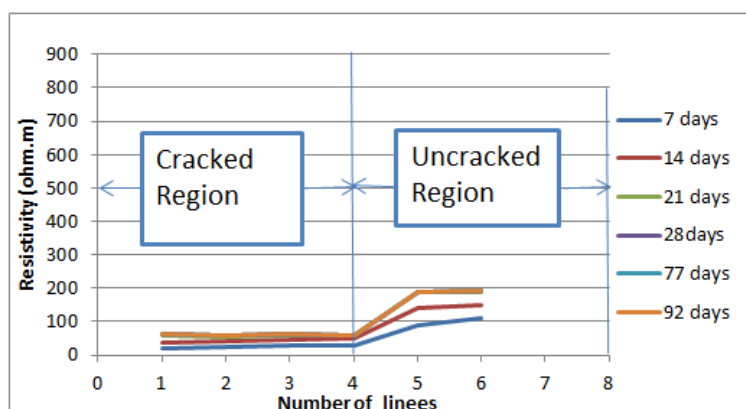


**Figure 17:** Square inner electrical resistivity measurements for cracked prism at direction parallel to the crack plane at different ages @ 25 mm electrode spacing

It was concluded that the percentage change in square inner electrical resistivity between cracked and uncracked prisms reached a value of 389% at the third line at age of 21 days as shown in Figure (18) at which

the direction of current perpendicular to the crack plane. The resistivity reached a minimum value at the fifth line at which the crack is away from the current direction.

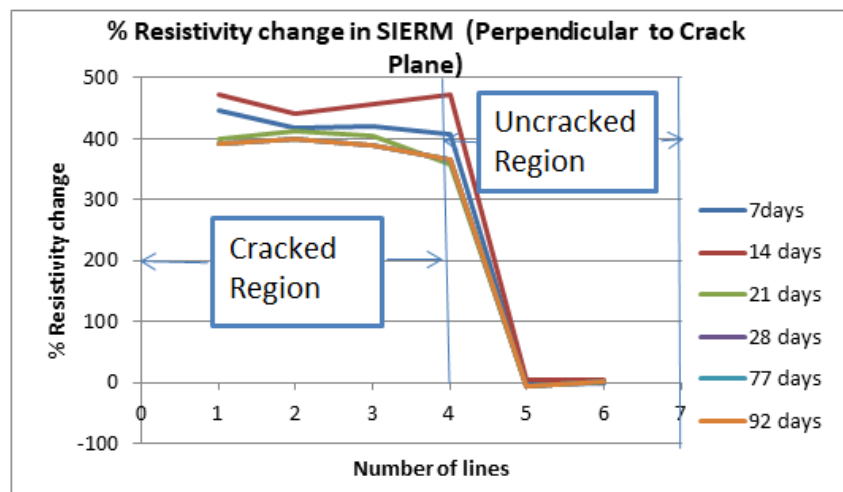


**Figure 18: Percentage change in SIERM between cracked and uncracked prisms at different ages (Perpendicular to the crack plane)**

It was concluded that the percentage change in square inner electrical resistivity between cracked and uncracked prisms reached a minimum value of -65 % at

the third line at age of 21 days as shown in Figure (19) at which the direction of current is parallel to the crack plane.

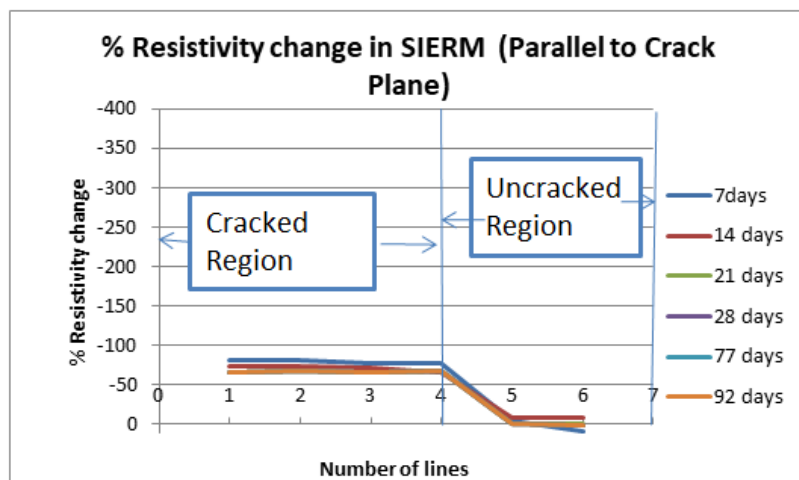


**Figure 19: Percentage change in SIERM between cracked and uncracked prism at different ages at 25mm electrode spacing  
(Parallel to the crack plane)**

The other parameter which can detect the presence of the crack is Decimal Logarithm Resistivity Anisotropy (DLRA) can be used only using 4 probes in square configuration measurement at which DLRA measure the current once in vertical direction and the other measurement is in horizontal direction and vice

versa. Decimal logarithm Resistivity An Isotropy (DLRA) can be calculated from equation (10).

$$DLRA = \log_{10} \left( \frac{Rv}{RH} \right) \text{ or } \log_{10} \left( \frac{RH}{Rv} \right) \dots \dots \dots \quad (10)$$

DLRA for uncracked prism reached a zero value as shown in Figure (20), because the resistivity is the same in the two perpendicular directions.

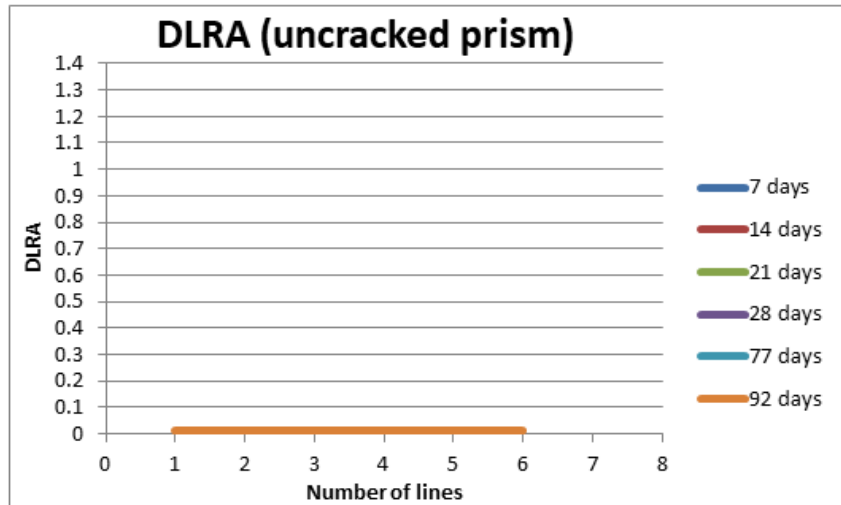


Figure 20: DLRA for uncracked prism (electrode spacing =25mm)

DLRA for cracked prism reached a value of 1.36, 1.3 and 1.2 at ages of 7, 14 and 21 days respectively at the third line as shown in the Figure (21) due to the presence of the crack. After the fourth line

the resistivity reached a minimum value due to the resistivity is the same in the two perpendicular directions.

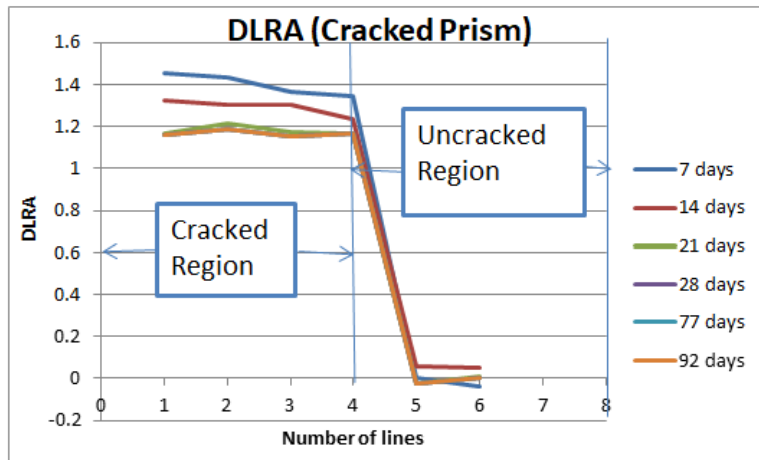


Figure 21: DLRA for cracked prism

#### 4. CONCLUSION

The heavy weight concrete used in this research and it is manufactured from hematite coarse aggregate which contains a large percentage of iron ores. Hematite coarse aggregate plays an important role in electrical resistivity. The two parameters which are used in detecting the manufactured cracks are the percentage change in electrical resistivity between cracked and uncracked prisms and Decimal Logarithm Resistivity Anisotropy (DLRA). The percentage change in LIERM between cracked and uncracked prisms in direction perpendicular to the crack at 7days and 21 days are 464%, 372% respectively. While the percentage change in SIERM between cracked and uncracked prisms in direction perpendicular to crack at 7days and 21 days are 420%, 389% respectively. Moreover, it was observed that the percentage change in square inner electrical resistivity reached a value of -

65% at age of 21 days at which the direction of current is parallel to the crack plane. In addition, the resistivity change gives a higher positive value of change when getting the change in resistivity between cracked and uncracked prisms in a direction perpendicular to the crack plane, while, the resistivity change gives a negative value of change when getting the change in resistivity between cracked and uncracked prisms in direction parallel to the crack plane. DLRA reached a value of 1.36 and 1.2 at ages of 7 and 21 days between resistivity perpendiculars to the crack plane to resistivity parallel to the crack plane for cracked prism. Inner electrical resistivity detects the damage specially the cracks. DLRA gives the direction of the crack inside the concrete prism. Inner Electrical Resistivity can be used easily to give continuous real time data about the health of RC structures especially the RC nuclear reactors.

## REFERENCE

- ELashkar, N. H., Elmasry, M. I. S., & Alasadi, M. F. A. (2012). Using internal electrical resistivity measurements as a tool for structural health monitoring. *Bridge Maintenance, safety, Management, Resilience and sustainability*- Biondini & Frangopol (Eds), Taylor and Francis Group, London.
- Elmasry, M. I. S., ElAshkar, N. H., & Alasadi, M. F. A. (2012). Damage Identification in RC Beams Using Internal Electrical Resistivity Measurements. *Journal paper in American society for civil Engineering*, pp.801-809.
- Ferreira, R. M., & Jalali S. (2010). NDT Measurements for the Prediction of 28-day Compressive Strength. *NDT & E International*, (43), 55-61.
- Gowers, K. R., & Millard S. G. (1999). Measurement of Concrete Resistivity for Assessment of Corrosion Severity of Steel Using Wenner Technique. *ACI Material Journal*, (96), 536-541.
- Lataste, J. F., Sirieix, C., Breysse, D., & Frappa, M. (2003). Electrical resistivity measurement applied to cracking assessment on reinforced concrete structures in civil engineering, *NDT & E International*, (36), 383-394.
- Madhavi, T. C., & Annamalai, S. (2016). Electrical Conductivity of Concrete. *ARPN Journal of Engineering and Applied Sciences*, 11(9), 5979-5982.
- McCarter, W. J., Starrs, G., Kandasami, S., Jones, R., & Chrisp, M. (2009). Electrode Configuration for Resistivity Measurements on Concrete, *ACI Materials Journal*, (106), pp. 258-264.
- Mehta, K. P., & Monteiro, P. J. (2006). Concrete Microstructure, Properties, and Materials, Electronic Book page 529-531.
- Morris, W., Moreno, E. I., & Sagues, A. A. (1996). Practical Evaluation of Resistivity of Concrete in Test Cylinders Using A Wenner Array Probe, *Cement and Concrete Research*, (26), 1779-1787.
- Ouda, A. S. (2014). Development of High-Performance Heavy Density Concrete Using Different Aggregates for Gamma-Ray Shielding .*Advances in civil, Environmental, and Materials Research* (ACEM 14).
- Polder, R. B. (2000). Electro chemical techniques for measuring metallic corrosion. *RILEM TC 154-EMC, Materials and Structures*, (33), 603-611.
- Shahroodi, A. (2010). Development of Test Methods for Assessment of Concrete Durability for Use in Performance-Based Specifications. Master science thesis.